Journal : SmallCondensed 10518 | Article No : 1999 | Pages : 30 | MS Code : 1999 | Dispatch : 20-8-2024

Bulletin of Earthquake Engineering
https://doi.org/10.1007/s10518-024-01999-6

ORIGINAL ARTICLE

Experimental behaviour of ductile diagonal connections for rack supported warehouses

Agnese Natali[1] · Francesco Morelli[1] · Cristian Vulcu[2] · Dimitrios Tsarpalis[3] · Dimitrios Vamvatsikos[3] · Walter Salvatore[1] · Benno Hoffmeister[2] · Ioannis Vayas[3]

Received: 1 March 2024 / Accepted: 13 August 2024

Abstract

Steel racking systems are widely adopted for storage purposes: they are thin-walled structures composed of consecutive trusses, connected with beams on which the palletized goods are stored. Their geometry and structural configuration strongly depend on market and operator necessities, and, in modern applications, racks can also function as the supporting structure of the warehouse itself in the form of Rack Supported or High-Bay Warehouses. With the increase of the overall geometric dimensions and the global weight of the stored material, the seismic action becomes more relevant for the design. Along these lines, the development and experimental testing of a dedicated seismic design approach for ductile steel racks is here presented, with particular attention to Rack Supported Warehouses. This approach exploits the ductility of trusses introduced via the plastic ovalization mechanism of the diagonal-to-upright connections while a tailored capacity design is used to assure the elastic behaviour of the rest of the structure and to keep the brittle failure mechanisms at bay.

Keywords Automated rack supported warehouses · Cold formed elements · Ductile connections · Plastic ovalization · Bearing failure

1 Introduction

Steel racks are structures dedicated to the storage of goods. Among the many types on the market (Tsarpalis et al. 2022), those designed to carry palletized goods are made of consecutive trusses connected by beams, on which the pallets are placed. Figure 1 shows the typical arrangements of the trusses, which are composed of two columns (so called

✉ Agnese Natali
agnese.natali@dici.unipi.it

[1] Department of Civil and Industrial Engineering, University of Pisa, Largo Lucio Lazzarino 2, 56122 Pisa, Italy

[2] Institute of Steel Constructions, Rheinisch-Westfälische Technische Hochschule Aachen, Mies-van-der-Rohe-Str. 1, 52074 Aachen, Germany

[3] Institute of Steel Structures, School of Civil Engineering, National Technical University of Athens, Zografou, Greece

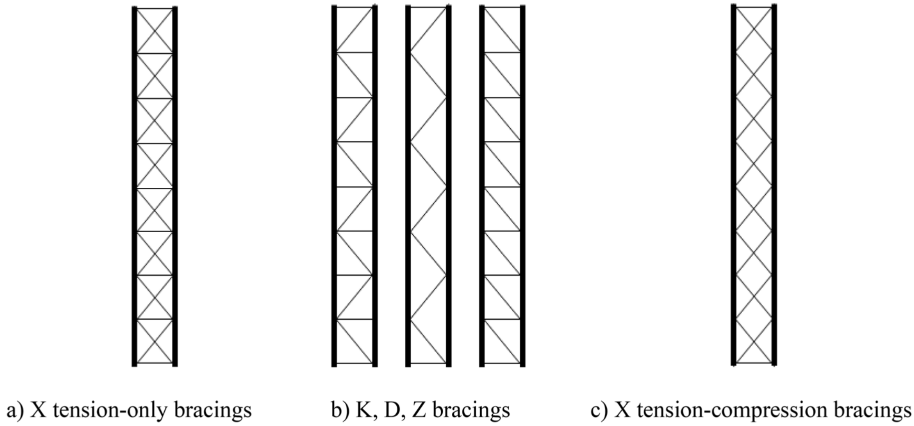

Fig. 1 Typical structural schemes for the trusses (CA direction)

"uprights") and diagonal braces. The steel racks comprise highly optimised, properly shaped thin-walled members aiming at minimizing the weight of the steel material used as well as the production and construction costs.

Racking systems are characterized by two principal structural directions: the transversal Cross Aisle one (CA) and the longitudinal Down Aisle one (DA) (Fig. 2, left). In the CA direction, the structure is made of grouped consecutive trusses separated by aisles. This aisle-spaces must remain free of any bracings to allow for placing the goods in the right stocking position. In the DA direction, the structure is a combination of semi-rigid frames assisted by trussed towers against lateral loads, i.e., designated bays where a bracing system is incorporated.

In their original use (named hereafter "ordinary"), racking systems are placed inside warehouses with the only structural function of carrying the goods. Several standards have been developed for their design in both static and seismic conditions (EN15512 and EN16681, (2016, 2020a)). With the increasing size and complexity of the storage facilities, an upgraded solution has been developed: steel racks are placed side by side and are

Fig. 2 Typical Cross Aisle (left) and Down Aisle (right) views of an RSW

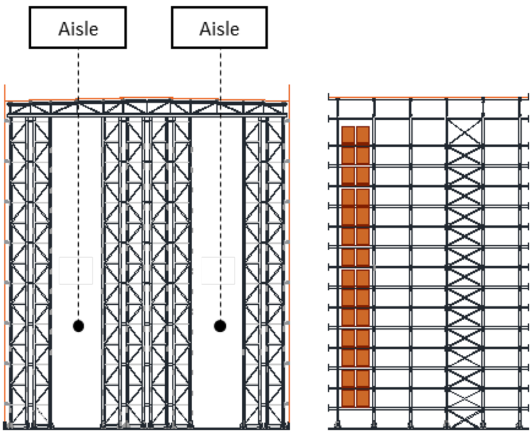

fully integrated into the warehouse, becoming its primary structural system while still carrying the palletized goods. These new structures are called Rack Supported Warehouses (RSWs) or High-Bay Warehouses. Despite additional structural functions and significantly increased loads, RSW racks inherit all the structural characteristics and design approaches developed for ordinary racks, leading to uncertain levels of safety, especially under seismic loading (Natali et al. 2022a).

Indeed, RSWs, being large structures made of assembled racking systems, should be designed for the safety level valid for comparable buildings, while considering all the structural, geometrical, and typological peculiarities of racks. However, the current standards for steel buildings (e.g., the Eurocodes) may be hardly applicable to RSWs due to their vast typological differences (especially for seismic applications (Caprili et al. 2018)), and at the same time, the standards for the ordinary racks may not guarantee achieving the necessary safety level. These two categories of standards may also be in conflict: for instance, the definitions and provisions for the applicable ductility classes (low, medium, high), as provided by EN16681(2016)—the European design standard for "ordinary" racks in seismic conditions—are different from the EN-1 provisions (2004, 2019, 2021).

The difficulties in the design of these structures are particularly evident in the CA direction, where the most common bracing arrangements for the trusses are the K, D, Z shapes (Fig. 1b) with diagonals designed to resist both tension and compression forces, in contrast to building-like X shapes (Fig. 1a) where diagonals in compression are assumed to buckle. Due to the necessity of a quick and easy assembly, diagonals are usually connected to uprights by single bolts, without employing gusset plates (Fig. 3). The trusses provide stiffness and resistance toward gravitational and lateral loads, but the absence of horizontal connections among the trusses and the structural performance of the thin-walled elements and of their connections make the application of EN1998-1 (2004) very difficult, in particular in case of dissipative seismic design approach (Caprili et al. 2018).

Starting from these considerations, this paper presents an experimentally validated design strategy specifically developed for the ductile seismic design of steel frames made

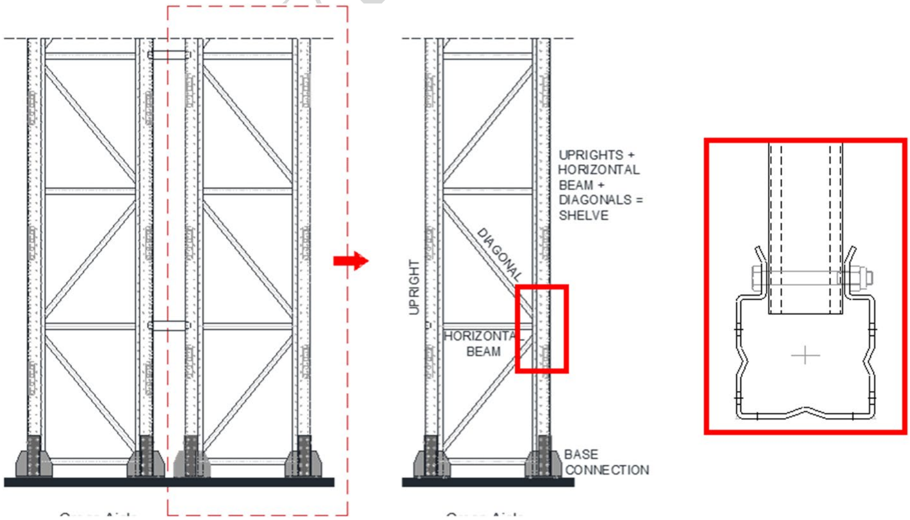

Fig. 3 Typical diagonal-to-upright connection

up of cold-formed profiles and single-bolted connections, like the typical frames in the CA direction of RSWs. The design strategy consists of controlling the ductility of the structure by allowing and tailoring the plastic ovalization in the diagonal-to-upright connections (termed accordingly "Plastic Ovalization Strategy"—POS). The theoretical development of the strategy, introduced in (Tsarpalis 2022), starts from the fact that most rack profiles are thin-walled, which allows the bearing failure to become the leading mechanism of their bolted connections, while brittle failure modes, involving net section, bolt shear, and diagonal tensile-buckling resistances, can be capacity-designed to become over-resistant with respect to bearing failure (Natali et al. 2022b). POS aims at activating the ductility of these connections when the elastic bearing resistance is exceeded. The potentiality of employing the ductility of plastic ovalization has already been investigated by Seleim and LaBoube (1996), Chung and Ip (2001), Lyu et al. (2019), and Cho et al. (2021), who provided, both numerically and in part experimentally, evidence on the ductility of this kind of mechanism, especially in the case of components made of the usual mild steel grades (i.e. S275), while it may be less efficient for high strength steels, and vary significantly based on the cooling methods adopted after the thermal treatment. However, these studies do not include considerations or experimental evidence for cold-formed thin-walled elements. In addition, to assure a similar behaviour of the connection when the diagonal is in tension versus in compression, a specific geometrical configuration of the diagonal has been proposed (Tsarpalis 2022) where an additional boltless hole is placed close to the connection (Fig. 4), creating another important endpoint for checking.

The study has been organized in the following three main phases: (i) application of POS to five case-study structures designed for medium/high seismicity; (ii) concept and execution of the experimental campaign in order to evaluate the actual behaviour of the connection after the application of the suggested design rules; (iii) discussion and analysis of the experimental results suggesting possible adjustments to the proposed strategy and setting the basis to define rules that drive structural choices.

2 The plastic ovalization strategy

The Plastic Ovalization strategy, as the name suggests, is based on the controlled formation of bearing failure mechanism in the diagonal bolt hole and allows driving the plastic deformations and damages induced by the seismic forces to this ductile part of the connection, only. Simultaneously, a tailored capacity design is applied to assure elastic behaviour of all other parts of the structure and to prevent any brittle failure mechanisms. As explained in detail in (Tsarpalis 2022) and (Natali et al. 2022c), POS aims at moderately increasing the overall ductility of the cross-aisle direction frames while keeping a simplified capacity design approach. The proposed capacity design rules are summarized as follows:

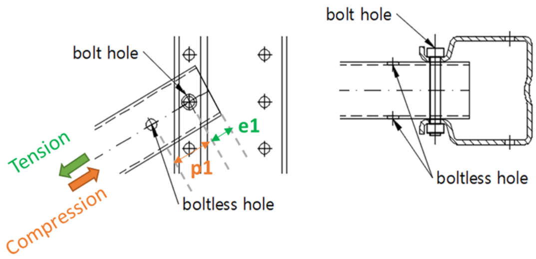

Fig. 4 Additional boltless hole to control bearing resistance in the diagonal in compression (adopted from (Tsarpalis 2022))

Journal : SmallCondensed 10518 | Article No : 1999 | Pages : 30 | MS Code : 1999 | Dispatch : 20-8-2024

(i) behaviour factor limited to a (provisional) maximum of 1.8. Indeed, not being sure of the actual level of ductility assured by plastic ovalization in cold formed elements, a precautionary value has been chosen for the behaviour factor, with the first aim of developing the strategy, proving the applicability to RSWs and with the will of calibrating the proper and hopefully higher value after the execution of experimental tests. The scheme adopted for the upright frame may be the K, Z or X tension-compression ones (Fig. 1), with diagonals designed to resist both tension and compression forces. In any case, all elements and components are designed ensuring that bearing failure will occur in the diagonal before any other mechanism in the CA plane.

(ii) Capacity design of the diagonal-to-upright connections. The bolt shear resistance $F_{v,Rd}$, the upright bearing resistance $F_{b,u,Rd}$, and the net section resistance $F_{n,Rd}$ shall be at least 20% higher than the diagonal bearing resistance $F_{b,d,Rd}$ per Eq. (1)–(3):

$$\boldsymbol{F}_{\boldsymbol{v},\boldsymbol{Rd}} \geq 1.20 \cdot \boldsymbol{F}_{\boldsymbol{b},\boldsymbol{d},\boldsymbol{Rd}} \tag{1}$$

$$\boldsymbol{F}_{\boldsymbol{b},\boldsymbol{u},\boldsymbol{Rd}} \geq 1.20 \cdot \boldsymbol{F}_{\boldsymbol{b},\boldsymbol{d},\boldsymbol{Rd}} \tag{2}$$

$$\boldsymbol{F}_{\boldsymbol{n},\boldsymbol{Rd}} \geq 1.20 \cdot \boldsymbol{F}_{\boldsymbol{b},\boldsymbol{d},\boldsymbol{Rd}} \tag{3}$$

(iii) Capacity design of the diagonal buckling resistance $N_{b,Rd}$. It shall be at least 20% higher than diagonal bearing resistance per Eq. (4):

$$\boldsymbol{N}_{\boldsymbol{b},\boldsymbol{Rd}} \geq 1.20 \cdot \boldsymbol{F}_{\boldsymbol{b},\boldsymbol{d},\boldsymbol{Rd}} \tag{4}$$

(iv) Uprights, horizontal beams, and all other elements besides diagonals shall be designed to remain in the elastic range for the design seismic action. This is achieved by adopting as design forces those due to non-seismic action plus those due to the seismic ones properly amplified (all the design rules are properly specified within (Tsarpalis 2022)), following the same philosophy adopted for non-dissipative elements of steel buildings, i.e. §6.6.3 of EN1998-1 (2004).

(v) Base connections shall be designed by amplifying the base forces by the adopted behaviour factor and also considering additional load combinations for gravitational loads, to maximize the uplift demand (Tsarpalis 2022).

The fundamental step of this strategy is the design of the diagonal connection. According to the previously highlighted hierarchies, it should be assured that the bearing resistance in the diagonal should be the first mechanism to occur for both tension and compression in the diagonal. In classical connections with single holes, however, the ultimate bearing resistance may vary depending on the direction of loading and the distance to edges of the connected member. For a profile in tension, the distance of the connection hole from the end section of the diagonal (e_1 parameter, Fig. 4) is the relevant geometrical parameter affecting the bearing resistance. In compression the distance is usually not relevant, so the bearing resistance may be higher than in tension. To achieve the same ultimate bearing resistance in tension and compression, a second boltless hole is placed close to the inner side of the connection. It controls (i.e., reduces) the bearing resistance in

Journal : SmallCondensed 10518	Article No : 1999	Pages : 30	MS Code : 1999	Dispatch : 20-8-2024

compression (Fig. 4). The adjustment to match the resistance in tension requires calibrating the distance (p_1 parameter, Fig. 4) between boltless and the connection hole. According to the aforementioned design rules the bearing resistance in compression shall not exceed the one in tension by more than 10%.

3 Design of the case study structures

Five RSW Case Studies (CS, A to E) were designed according to the POS rules by five rack manufacturers. The design focused on the CA frames, which consist of consecutive upright trusses, as presented in Fig. 3. These selected case study structures were two Multi Depth (MD) and three Double Depth (DD) warehouses, which represent the main structural typologies of RSWs: the former is characterized by consecutive and reciprocally connected upright trusses in the CA direction (Fig. 5), while in the latter the upright trusses are grouped and separated by aisles, with a maximum of two “depths” (i.e., able to accommodate two pallets) available from each side of the aisle (Fig. 6). For each structural type, the global geometry, height, and number of load levels were the same, as shown in Fig. 5 for the MD ones and in Fig. 6 for the DD ones. Pallet weight, external actions, and load combinations were also defined to be common, and the POS rules were adopted by all the designers in order to have comparable solutions. The design parameters free to select were the structural scheme for the diagonal elements constituting the upright trusses, the cross sections of the main profiles, and the configuration of the connections.

Table 1 gathers the main geometrical parameters of the case study structures, Fig. 7 shows the terminology for the typical cold-formed sections used in racks, while Table 2 gathers the characteristics of the most stressed connections, providing also the resistances relevant to the possible failure mechanisms. The tables do not provide the exact details of the cross-section geometries, as these data constitute sensitive information owned by the producers; indeed, their design philosophies vary significantly, as evidenced by the diverse solutions adopted for the element cross sections. In any case, all the relevant parameters for the comprehension of the applications and data post-process are provided.

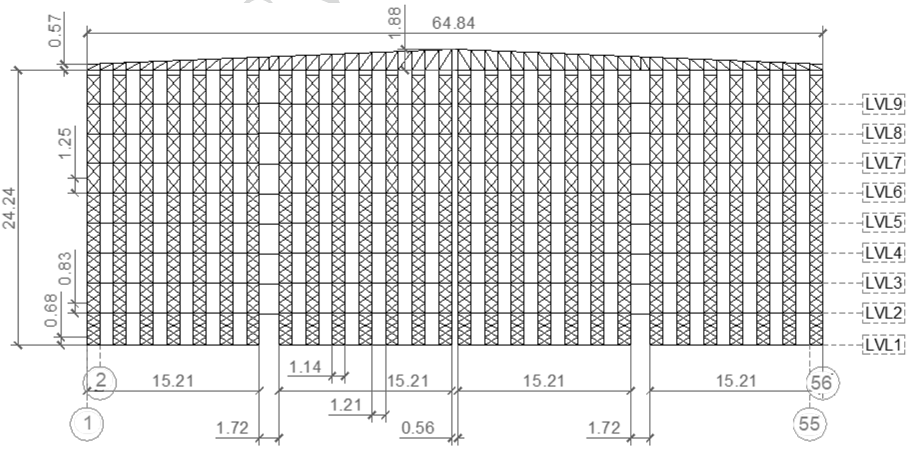

Fig. 5 Geometry of the CA frame of the MD case studies (dimensions in m—diagonal layout can change). LV is “load level”

Journal : **SmallCondensed 10518**	Article No : **1999**	Pages : **30**	MS Code : **1999**	Dispatch : **20-8-2024**

Fig. 6 Geometry of the CA frame of the DD case studies (dimensions in m). LV is "load level"

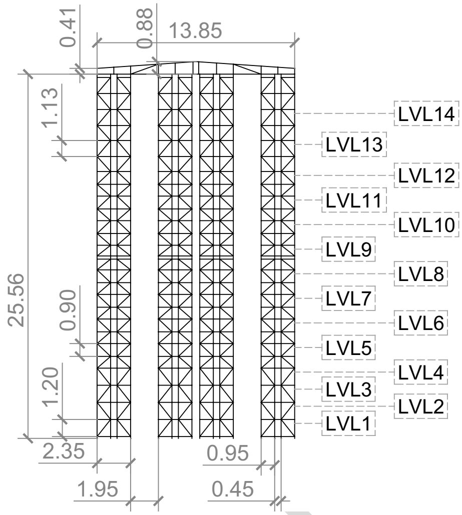

Table 1 Global geometric characteristics of the Case Study structures

	CS A	CS B	CS C	CS D	CS E
Structural type	MD†	DD†	DD	DD	MD
Diagonal scheme	K‡	K	K	K	X‡
Diagonal-to-upright connection	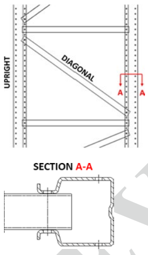	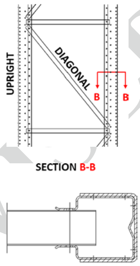	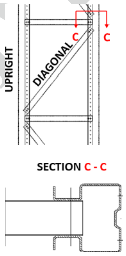	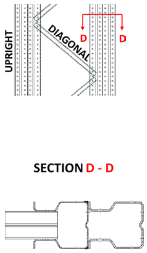	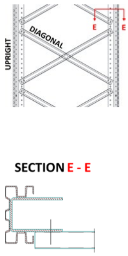

†*DD* Double Depth, *MD* Multi Depth

‡For scheme K see Fig. 1b; for scheme X see Fig. 1c

Fig. 7 Terminology of typical cold-formed sections used in racks

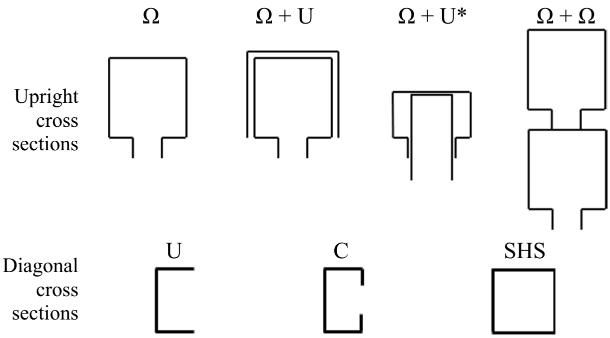

Journal : SmallCondensed 10518	Article No : 1999	Pages : 30	MS Code : 1999	Dispatch : 20-8-2024

Table 2 Main geometric characteristics and resistance properties of the connections in the bottom part of the Case Study structures

Characteristics of the connection		CS A	CS B	CS C	CS D	CS E
Diagonal	Thickness [mm]	3.0	2.0	3.0	3.0	1.5
	e_1[mm]	25	29	25	40	20
	p_1[mm]	35	39	35	49	30
	Steel grade	S275J0H	S350GD	S235	S355	S280GD
	f_{yk}/f_{uk} [MPa]	275/430	350/420	235/360	355/510	280/360
Upright	Thickness [mm]	5	4	3.5	2.5	4
	e_1[mm]	–	–	–	38	–
	p_1[mm]	–	–	–	–	–
	Steel grade	S500MC	S350GD	S420	S500MC	S235JR
	f_{yk}/f_{uk} [MPa]	500/550	350/420	420/480	500/550	235/360
Number of diagonals per connection		1	1	1	2	1
Number of shear planes		2	2	2	1	1
bolt – diameter and class		M12 8.8	M12 8.8	M12 8.8	M12 8.8	M12 8.8
Holes diameter [mm]		13	13	13	13	13
$F_{b,d,Rd+}$[kN]		43.00	32.48	36.00	36.72	7.20
$F_{b,d,Rd-}$[kN]		44.72	33.60	37.44	36.72	7.56
$F_{b,u,Rd+}$[kN]		132.00	80.64	80.64	33.00	34.56
$F_{b,u,Rd-}$[kN]		132.00	80.64	80.64	33.00	34.56
$F_{b,u,Rd+}/F_{b,d,Rd+}$		3.07	2.48	2.24	**0.90**	4.80
$F_{b,u,Rd-}/F_{b,d,Rd-}$		2.95	2.40	2.15	**0.90**	4.57
$F_{v,Rd}$[kN]		65.14	65.14	65.14	32.57	32.57
$F_{v,Rd+}/F_{b,d,Rdmin}$		1.51	2.01	1.81	**0.89**	4.52
$F_{n,Rd}$[kN]		165.64	82.79	133.05	115.25	44.39
$F_{n,Rd}/F_{b,d,Rd+}$		3.85	2.55	3.70	3.14	6.17

Table 2 also provides the resistance values of the possible mechanisms of the connection, calculated by employing the formulas of EN1993-1-3:2019, Table 10.5 (2019), which are given as follows:

$$F_{b,Rd} = \frac{2.5 \cdot \alpha_b \cdot k_t \cdot \mathrm{d} \cdot \mathrm{t} \cdot f_u}{\gamma_{M2}} \tag{5}$$

$$\alpha_b = \begin{cases} \min\left(1.0; \frac{e_1}{3\cdot \mathrm{d}}\right) & \text{for tension} \\ \min\left(1.0; \frac{p_1}{3\cdot \mathrm{d}} - 0.25\right) & \text{for compression} \end{cases} \tag{5a}$$

$$k_t = \begin{cases} \frac{(0.8\cdot \mathrm{t}+1.5)}{2.5} & \text{for} \quad 0.75 \le t \le 1.25 \quad \text{mm} \\ 1.0 & \text{for} \quad t > 1.25 \quad \text{mm} \end{cases} \tag{5b}$$

Journal : SmallCondensed 10518 | Article No : 1999 | Pages : 30 | MS Code : 1999 | Dispatch : 20-8-2024

$$F_{n,Rd} = \frac{A_{net} \cdot f_u}{\gamma_{M2}} \cdot \left[1 + 3 \cdot k_{num} \cdot \left(\frac{d_0}{u} - 0.3\right)\right], \quad \text{but} \quad 1 + 3 \cdot k_{num} \cdot \left(\frac{d_0}{u} - 0.3\right) \leq 1 \tag{6}$$

$$k_{num} = \frac{\text{number of bolts at the cross section}}{\text{total bolts in the connection}} \tag{6a}$$

$$u = 2 \cdot e_2, \quad \text{but} \quad u \leq p_2 \tag{6b}$$

$$F_{v,Rd} = \frac{0.6 \cdot A_s \cdot f_{ub}}{\gamma_{M2}} \tag{7}$$

where: d is the bolt diameter; t is the thickness of the profile; f_u is the ultimate tensile strength of the profile material; γ_{M2} equal to 1.25 is the safety coefficient for connections; e_1 is the end distance from the centre of the bolt to the adjacent end-section of the profile in the direction of load; A_{net} is the net cross-section area of the profile at the connection, d_0 is the diameter of the bolt hole; e_2 the edge distance from the centre of the bolt to the adjacent edge of the profile in the direction perpendicular to the direction of load; A_s is the equivalent area of the bolt; f_{ub} is the ultimate tensile strength of bolts.

Within Table 2, the bearing resistance $F_{b,Rd}$ has been calculated for both diagonal ($F_{b,d,Rd}$) and upright side ($F_{b,u,Rd}$), and in both cases for tension (+) and compression load (−). For most upright profiles, $F_{b,u,Rd}$ was calculated by assuming that the maximum bearing resistance can be attained. Indeed, the edge distance parameters e_1 and p_1 in these members are typically high enough to result in α_b equal to 1.0 in Eq. (5). It also can be noticed that the capacity design rules (i) to (iv) have been respected (as indicated in the same Table 2 by the resistance ratios being greater than 1.0), except for case study D failure to adhere to the capacity design rules may disrupt the intended behaviour, as was also observed in the experimental campaign of this case study.

A preliminary numerical investigation through response history non-linear analyses was carried out to evaluate the global and local performance of the case-study structures designed according to the POS philosophy (Tsarpalis 2022). The numerical models of the case study structures were developed by adopting a simplified approach that allows to reduce the number of elements and degrees of freedom (this approach is described within (Tsarpalis et al. 2021)). In general, the core of the method is substituting all the upright trusses with an equivalent truss made of beam elements, and simulating the expected behaviour of connection trough non-linear springs that connect the diagonals of the truss to the uprights. All the developed models captured the non-linear behaviour of the diagonal-to-upright connections according to the force-deformation curves provided by prEN 1993-1-8:2021 (2021) for bearing resistance. As shown by (Tsarpalis 2022), the results of the analyses confirm that on average, the re-designed structures guarantee the desired behaviour up to a probability of exceedance of 10% in 50 years, which is beyond the design level selected for these case studies (20% in 50 years). Indeed, even if limited global and local overstrength was assumed by applying the proposed POS design rules, the redesigned racks demonstrated the desired behaviour at the design level with only few records leading to brittle failure modes. These highly promising results necessitate the experimental validation described in the following sections, to verify the validity of the assumed behaviour factor of 1.8 adopted in this preliminary definition of the design strategy. While according to (Tsarpalis 2022) higher values seem perfectly achievable, a comprehensive validation of a code-level value would require even further numerical and testing campaigns (Tsarpalis et al. 2020; Vamvatsikos et al. 2020).

4 Concept and execution of the experimental campaign

According to the POS, a limited energy dissipation and ductility demand is expected in the diagonal-to-upright connection after exceeding the bearing resistance of the diagonal. To avoid a resistance reduction of the vertical loading resisting system, the upright is designed to exclude any damage, including plastic ovalization. To have a full characterization of both the ductility-providing element—the diagonal—and the upright-to-diagonal connection assembly, two sets of tests are performed, namely the *Local tests* and the *Assembly tests*.

The *Local tests* aim at assessing the actual bearing resistance of the connection without any interference from other failure modes. To this purpose, short diagonals are tested under monotonic tensile and compressive loads for different positions of the boltless and bolted holes, as defined by dimensions e_1 and p_1 within Fig. 8a. For each case study structure, one diagonal is selected from the bottom part of the upright trusses, where the diagonals are subjected to the highest forces under horizonal actions. The geometrical characteristics and resistance values of the tested elements and connections are gathered in Table 2.

In the *Assembly tests*, the same diagonal profiles are tested in their actual configuration, i.e., each diagonal has the full length and are connected to the upright trusses as designed in the case-study structures (Fig. 8b and Table 1). Each configuration is tested four times: one under monotonic tensile load, one under monotonic compression load, and two under cyclic load. All the tests are displacement controlled, for a total of 20 tests (5 configurations × 4 tests/configuration). The purpose is to observe the response of the whole assembly and assess whether the safety factor for the design of the over-resistant components is sufficient to guarantee the desired behaviour: bearing strength of the diagonal connection (diagonal side) should be reached first, while other failure modes should be prevented (this

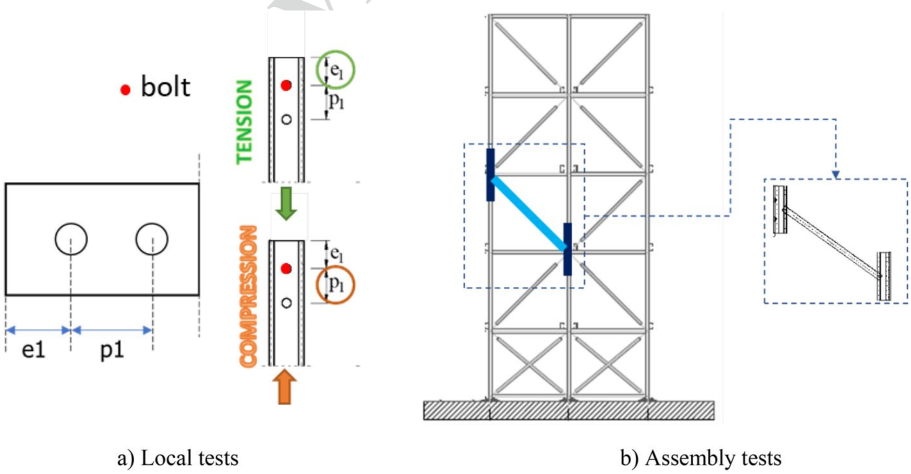

Fig. 8 **a** Local tests: varying parameters for the different configurations of the tested components; **b** Assembly tests: component assembly and configuration

Journal : SmallCondensed 10518 | Article No : 1999 | Pages : 30 | MS Code : 1999 | Dispatch : 20-8-2024

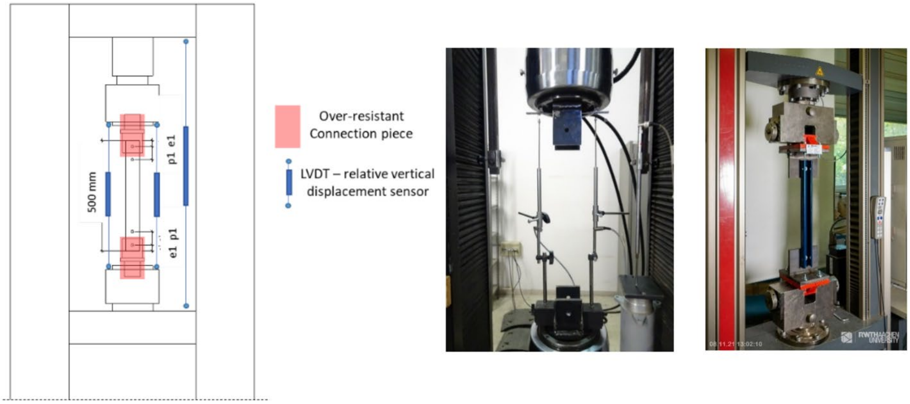

(a) (b) (c)

Fig 9 **a** Schematic view of the test set-up for the universal machine local tests, and the universal devices at the laboratories of the **b** University of Pisa and **c** RWTH Aachen

Table 3 Configuration of the diagonals for the local tests

Case study structure		A	B	C	D	E
Diagonal cross-section shape		SHS	C	SHS	C	C
Thickness [mm]		3.0	2.0	3.0	3.0	1.5
Hole diameter		Φ13	Φ13	Φ13	Φ13	Φ13
Bolt diameter and class		M12 8.8	M12 8.8	M12 8.8	M12 8.8	M12 8.8
e_1/ p_1 †	1–tensile load	**25**/35	**29**/39	**25**/35	**40**/49	**20**/30
	2–compression load	25/**35**	29/**39**	25/**35**	40/**49**	20/**30**

† Bold font indicates the dimension that governs bearing strength in each specimen

includes shear failure of bolts, damage in upright due to bearing, failure of diagonal net section, and buckling of diagonal in compression).

4.1 Local tests: set-up, components and loading protocol

The Local tests are executed by adopting the test set-up shown in Fig. 9a; the two different universal testing machines employed appear in Fig. 9b,c. Each diagonal is 500 mm long and connected at each end by a single bolt to an over-resistant element to confine damage only in the diagonal. Displacement sensors are placed to measure the relative displacements of the end sections of the diagonal. The load is directly measured through the universal machine.

Table 3 gathers the characteristics of the tested components. In all tests the load is increased until failure of the component. Dimensions e_1 and p_1 are selected to satisfy the requirements set by the POS design strategy, as listed in Sect. 2. The tests also allow verifying the capability of controlling the bearing resistance in compression with the addition of the boltless hole: this is assessed by evaluating the ratio between experimental bearing resistances in compression and tension, which, according to the POS rules, shall not be higher than 1.10.

4.2 Assembly tests: set-up, components and loading protocols

Figure. 10 shows the test set-up adopted for the Assembly tests: the load is applied through a hydraulic actuator, fixed at one end and connected to a pinned column at the other end. Looking at Fig. 10, the profile representing the left upright is connected to the pinned column, and the right upright is connected to a base anchorage that is fixed to the basement of the set-up. The pieces used to connect the specimens to the set-up are adjustable to fit the geometries of the different specimens. For each test, load is measured by a loading cell, and a set of displacement sensors are placed to monitor the deformation of the diagonal. In particular, one displacement sensor directly measures the global deformation of the diagonal between the two connection bolts (Fig. 10). Additionally, two sensors are positioned to directly measure the deformations related to plastic ovalization at the upper and lower connections, respectively. Further displacement sensors are placed to indirectly control the previous values and to ensure that all components of the set-up are functioning properly during the tests.

Tables 4 and5 gather the characteristics of the specimens (respectively diagonal and upright pieces). The length of the diagonals, their inclination and connections are the same, as extracted from the upright trusses designed in the case studies. The uprights-sections are 500 mm long, which is the necessary length to allow the connection of the assembly to the test set-up. The geometry of the test set-up has been set to meet the different geometries of the assembly and of the upright profiles.

Monotonic tension and compression tests are performed by increasing the applied load till failure of the diagonal is observed. Two quasi-static cyclic tests are executed for each specimen, with two different displacement protocols. The first is the one defined by ECCS (1986). The *ECCS protocol* is based on the e_{y+} and e_{y-} values determined from the monotonic tension and compression tests. These values are derived from the obtained

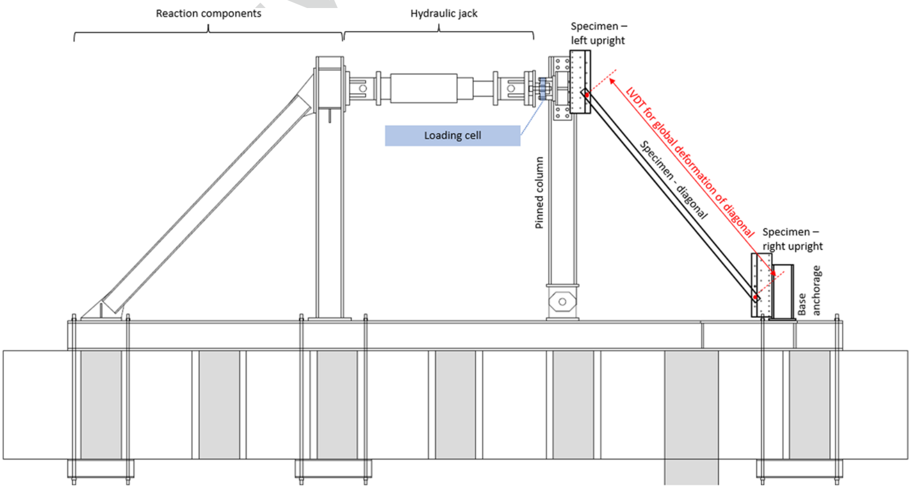

Fig. 10 Test set-up adopted by the University of Pisa for the Assembly tests

Journal : SmallCondensed 10518	Article No : 1999	Pages : 30	MS Code : 1999	Dispatch : 20-8-2024

Table 4 Configuration of the POS diagonals for the Assembly tests

	Cross-section shape	Thickness [mm]	Hole diameter [mm]	e_1[mm]	p_1[mm]	Bolt diameter and class	Length [mm]
A	SHS	3.0	13	25	35	M12 8.8	1252
B	C	2.0	13	29	39	M12 8.8	1428
C	SHS	3.0	13	25	35	M12 8.8	1324
D	C	3.0	13	40	49	M12 8.8	830
E	C	1.5	13	20	30	M12 8.8	1198

Table 5 Configuration of the POS uprights for the Assembly Tests. For the cross-section shape refer to Fig. 7

	Cross-section shape	Thickness [mm]	Hole diameter [mm]	Bolt diameter and class	Length [mm]
A	Ω	5.0	13	M12 8.8	500
B	Ω+U	4.0+5.0	13	M12 8.8	500
C	Ω	3.5	13	M12 8.8	500
D	Ω+Ω	4.0+2.5	13	M12 8.8	500
E	Ω+U*	2.0+4.0	13	M12 8.8	500

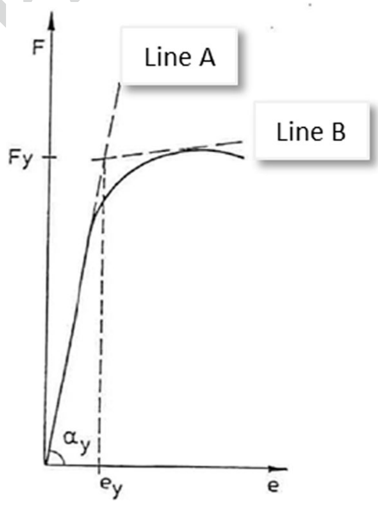

Fig. 11 Definition of e_y according to ECCS (1986)

force-displacement curves, as the displacement corresponding to the intersection of line A (tangent to the origin of the curve) and line B (line with a slope which is one tenth of the slope of line A) as shown in Fig. 11. Figure. 12a shows the definition of the (unitless) protocol as a multiple of e_{y+} and e_{y-}.

The second protocol is designed to be *damage-consistent*, replicating the observed statistics of cycles that lead to ovalization (i.e., damage) of the bolt hole. It is derived by conducting statistical analysis on the seismic response of a realistic double-depth RSW

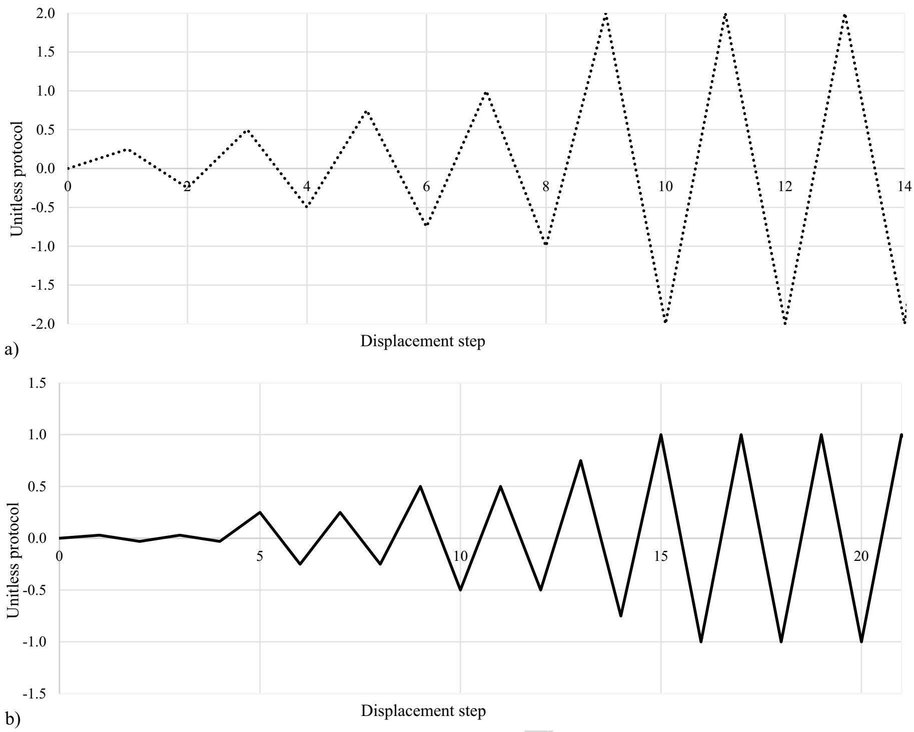

Fig. 12 Unitless **a** *ECCS* and **b** *damage-consistent* displacement protocols for the Assembly cyclic tests

designed according to the POS. To this end, the results of the 30 response history analyses carried out by Tsarpalis et al. (Tsarpalis 2022) are used, and for each analysis the force-displacement diagram of a zero-length element representing the upright-to-diagonal connection is post-processed to count the number of inelastic cycles, i.e., the number of times the bolt hole further ovalizes due to the bearing failure. These results are statistically analyzed to derive the loading protocol shown in Fig. 12b. The overall goal of this protocol is to avoid the generic repetition of a given number of cycles until failure, enforcing higher cyclic degradation before ultimate failure, and instead replicate the expected number and amplitude of cycles enforced in a realistic seismic loading situation, as also employed for the collapse assessment of steel structures (Suzuki and Lignos 2019).

5 Experimental results

In this section, the results obtained from both Local and Assembly tests are shown and discussed for each profile. Table 6 provides the material characterization from the execution of tensile coupon tests, which are also used to compare the design and experimental values of bearing resistance. The data for the type D profile are not available; therefore, all further analyses and comparisons described in the following for type D are carried out considering the nominal values of the resistance. The material property that is relevant for the evaluation of the bearing resistance is the nominal tensile strength f_u associated to the material

Journal : SmallCondensed 10518 | Article No : 1999 | Pages : 30 | MS Code : 1999 | Dispatch : 20-8-2024

Table 6 Material characterization of the diagonal elements

Diagonal type	Cross-section shape	Thickness (design) [mm]	Steel grade	Nominal values			From coupon tensile tests			R_{eH}/f_{yk}	R_m/f_u
				f_{yk} [N/mm^2]	f_u [N/mm^2]	A_{min} [%]	R_{eH} [N/mm^2]	R_m [N/mm^2]	A [%]		
A	SHS	3.0	S275J0H	275	430	20	340	423	30	1.24	0.98
B	C	2.0	S350GD	350	420	16	480	501	25	1.37	1.19
C	SHS	3.0	S235	235	360	19	383	457	29	1.63	1.27
D	C	3.0	S355	355	510	26	–	–	–	–	–
E	C	1.5	S280GD	280	360	18	530	541	10	1.89	1.50

classification and the corresponding experimental value R_m as derived from the coupon tests. The values of f_u reported in the table are the minimum ones associated to the respective steel grade. The R_m ones resulting from the coupon tests are generally higher than f_u, except for the type A diagonal, where R_m is slightly lower (-1.7%). The type E diagonal is characterized by high and quite close values of both the experimental upper yielding, R_{eH}, as defined by EN ISO 6892 (2020b), and tensile, $R_{m,}$ strength, meaning that the material may have already experienced plastic deformations (e.g. due to the cold-forming shaping process). This is suggested also by the reduced value of elongation percentage after fracture, A, if compared to the other materials and to the minimum requested from the steel classification, A_{min}.

5.1 Local tests

The force-displacement curves and the final state of the specimens are given in Fig. 13 for the tensile tests and Fig. 14 for the compression tests. In these figures, "displacement" corresponds to the total lengthening of the diagonal as measured by the displacement sensors (Fig. 9). To allow for a useful comparison with the resistances calculated for design assessments, the figures also report the values of the diagonal bearing resistance in tension and in compression, respectively named $F_{b,d,Rd}+$ and $F_{b,d,Rd-}$, calculated according to prEN1993-1-3:2019 (2019) (Eq. 5) by adopting the characteristic value of the ultimate tensile strength ($f_u = f_{uk}$) but not taking into account the safety factor γ_{M2} ($\gamma_{M2} = 1.00$).

All profiles demonstrated behaviours with similar traits, even if having differences in the shapes/thicknesses and in the final configurations based on the distances of the connection hole from the free edge (for the tensile tests) or from the boltless hole (for the compression tests). For the tensile tests, the force-displacement curves and the final state of the specimens after the tests (Figure 13a, b, respectively) show that all the connections experience plastic deformations. After large deformation of the holes, different failure modes can be observed: in the case of A and C elements, tearing of the end section occurs; in the case of B and D profiles, the large deformation of the hole is accompanied by local buckling of the plate. In the case of E profile, both types of failure can be clearly observed.

A similar global behaviour can also be observed among the compression tests (Fig. 14b), comprising plastic ovalization of the hole and local buckling of the plate in compression due to contact with the bolt. In cases A, C, and D tearing of the web occurs after buckling, while in the case B and E large plastic deformations are accompanied by buckling only.

The analysis of results highlights that the bearing resistance evaluated through the approach proposed by the current Eurocodes are not fully in line with the experimental outcomes. This difference can be observed for both the tensile and compression tests, with a more evident difference in the latter case. To better clarify this aspect, Table 7 reports the experimental bearing resistances in tension and compression ($F_{b,exp}$, lines 5 and 6 of the table) and the design ones, the latter evaluated considering both the nominal f_{uk} and experimental R_m values of the tensile strength ($F_{b,d,Rd}$, lines 7–10 of the table). A graphical rapresentation of these values is also provided within Fig. 15, so to have their immediate comparison. In particular, the values of $F_{b,d,Rd}$ evaluated using the experimental R_m values (line 9–10 of the table) allow a design estimation net of the influence of material over-resistance. In this way, comparing these last values with the experimental ones ($F_{b,exp}$ / $F_{b,d,Rd}$ ratios, see line 13 of the table), it is possible to observe the influence of only the connection geometry on the bearing resistance (in the design values, these effects are considered through the α_b parameter (Eq. 5)) without

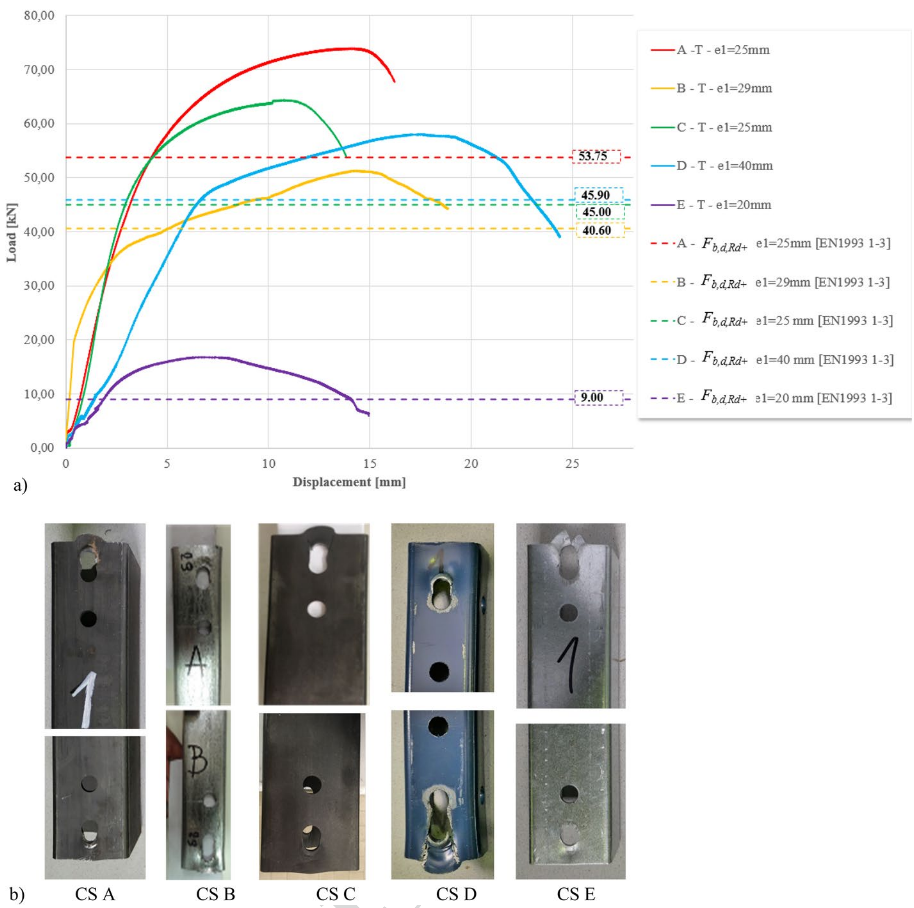

Fig. 13 *Local tests:* **a** Force-displacement curves (solid lines) versus code predictions accounting for actual material strength (dashed lines), and **b** damaged configuration under tensile load (T)

taking into account the influence of the material properties. For both for compression and tension, these ratios are always major than one, highlighting the design formula may not consider possible additional resisting mechanisms related to the geometrical configuration of the connection and of the element. In particular:

- In the case of tension, this can be due to the geometrical configuration of the cross section and related "border effects" due to the limited distance of the connection hole to the lateral borders of the profile.
- In the case of compression, where the ratios are significantly higher than the tension ones, in addition to the "border effects", it should be pointed out that the formula for the α_b parameter included in the Eurocodes may not be well calibrated for the "boltless" status of the internal hole. This can be observed also by the ratios between tension and compression experimental values and the same ratios with the design ones (line 14 of the table): from the design previsions, the values are quite close, while

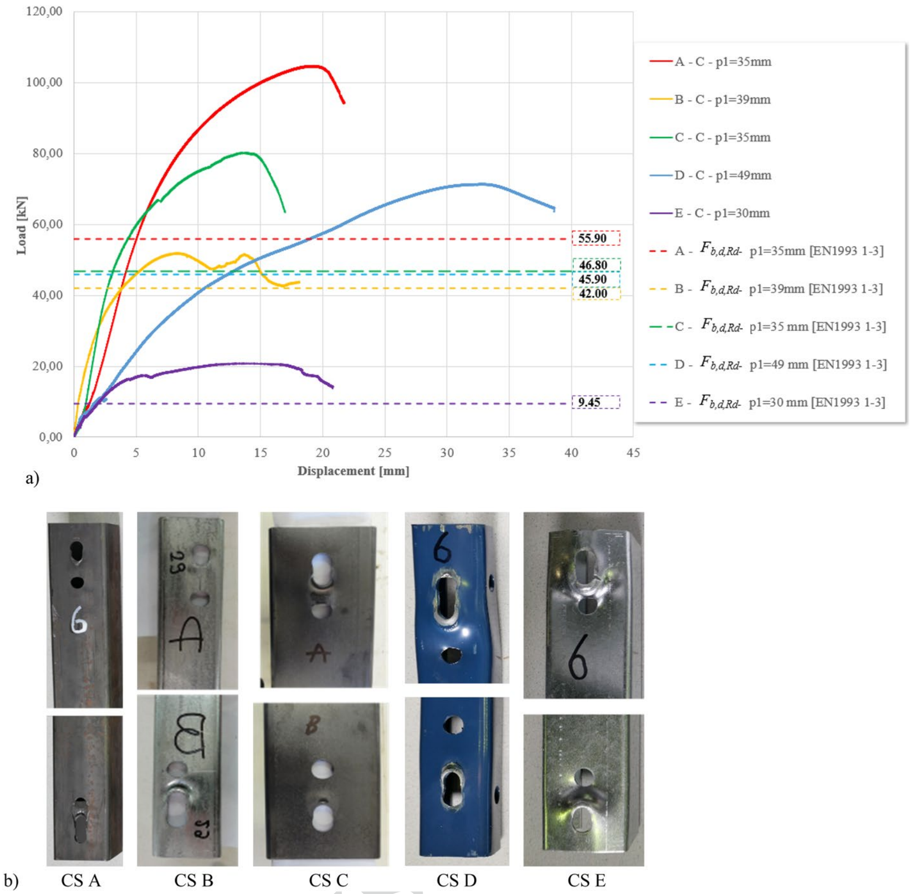

Fig. 14 *Local tests*: **a** Force-displacement curves (solid lines) versus code predictions accounting for actual material strength (dashed lines), and **b** damaged configuration under compression **C** load

the experimental evidence proves the relevant under-estimation of the bearing resistance in compression by adopting the design formula.

With a wider sample, it could be possible to extend these considerations and to calibrate the value of α_b more accurately, also by correlating the failure modes with the e_1 and p_1 distances. A better calibration of α_b could also lead to a better evaluation of the effective bearing resistance of bolted thin-walled elements, especially under compression load and bolt-less inner holes, that should be useful especially in case of capacity design applications (as in this case) (Fig. 15).

5.2 Assembly tests

The *Assembly Tests* are performed on the sub-system consisting of a diagonal element connected to two upright segments, whose configuration respects the actual geometry of the

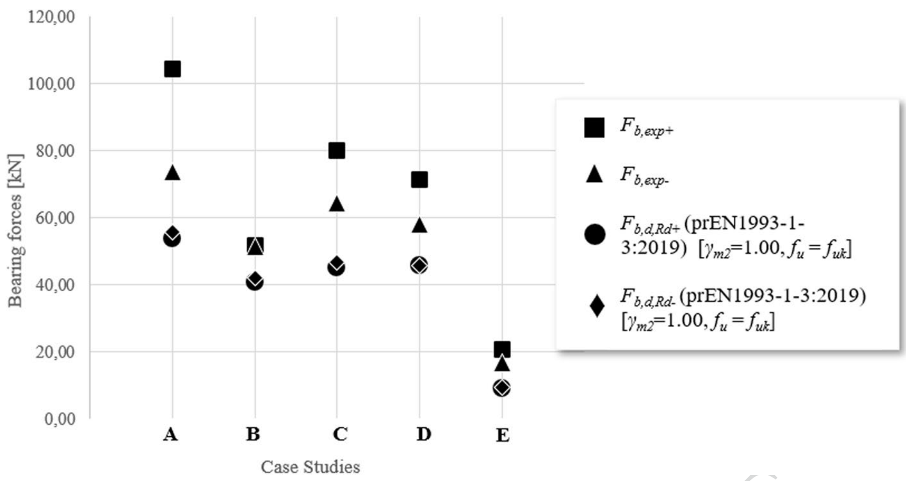

Fig. 15 Graphical comparison of the bearing resistance from tests and from applying the formula of prEN1993-1-3:2019 (2019) (Eq. (5))

upright trusses (Fig. 8b). The outcomes of the monotonic (tension and compression) and cyclic load tests are presented, compared, and discussed in the following in terms of force-displacement curves and observations on the failure modes.

5.2.1 Monotonic tests

The force-displacement curves obtained for all assemblies and for both tensile and compression monotonic load are shown in Fig. 16, where they are also compared with the monotonic curves from the *local tests* in order to highlight the influence of the full length of the diagonal and of the upright. Displacements are measured between the bolts of the diagonal connection (Fig. 10), thus representing the deformations only occurring in the diagonal member. Only for CS B, due to the lack of local measurements, the displacements are derived from an indirect measure (movement of the hydraulic jack), resulting in an apparent difference in terms of stiffness, see Fig. 16b.

In general, for both the tensile and compression assembly tests there is a good correlation with the behaviour observed in the local tests in terms of stiffness and resistance. This highlights that respecting the proposed POS rules and properly proportioning the structural elements and connections, the influence of the other components of the assembly can be limited and the desired failure mechanism can be developed, thus concentrating damage, plasticity, and dissipation only in the connection. The only relevant non-compliance can be observed in CS D, which is characterized by a design mistake already previously highlighted (see Table 2, ratios $F_{b,u,Rd+}/F_{b,d,Rd+}$ and $F_{b,u,Rd-}/F_{b,d,Rd-}$, where it can be noticed that the over-resistance of upright bearing resistance $F_{b,u,Rd}$ with respect to diagonal bearing resistance $F_{b,d,Rd}$ has not been guaranteed, being their ratio minor than 1.00, while the POS design rules require this ratio to be major than 1.20).

This led to a quite similar bearing resistance for the diagonal and for the upright in the design phase, which obviously influenced the behaviour observed in the Assembly tests, where plastic ovalization is placed both diagonal and upright sides. For this reason, CS D is analysed separately afterwards.

Table 7 Comparison of bearing resistance values from tests and from prEN1993-1-3:2019 (2019) (Eq. (5)), and comparison among tensile and compression bearing resistance

		Parameter	CS A	CS B	CS C	CS D	CS E
1		e_1	25	29	25	40	20
2		α_b (e_1)	0.69	0.81	0.69	1.00	0.56
3		p_1	35	39	35	49.00	30
4		α_b (p_1)	0.72	0.83	0.72	1.00	0.58
5		$F_{b,exp+}$ [kN]	73.85	51.31	64.37	57.99	16.77
6		$F_{b,exp-}$ [kN]	104.59	51.79	80.13	71.31	20.74
7		$F_{b,d,Rd+}$ [kN] (EN1993-1-3) [$\gamma_{M2} = 1.00, f_u = f_{uk}$]	53.75	40.60	45.00	45.90	9.00
8		$F_{b,d,Rd-}$ [kN] (EN1993-1-3) [$\gamma_{M2} = 1.00, f_u = f_{uk}$]	55.90	42.00	46.80	45.90	9.45
9		$F_{b,d,Rd+}$ [kN] (EN1993-1-3) [$\gamma_{M2} = 1.00, f_u = R_m$]	52.68	48.31	57.15	–	13.50
10		$F_{b,d,Rd-}$ [kN] (EN1993-1-3) [$\gamma_{M2} = 1.00, f_u = R_m$]	54.78	49.98	59.44	–	14.18
11	Design values $f_u = f_{uk}$ vs $f_u = R_m$	$F_{b,d,Rd+}$ [$\gamma_{M2} = 1.00, f_u = R_m$] / $F_{b,d,Rd+}$ [$\gamma_{M2} = 1.00, f_u = f_{uk}$]	0.98	1.19	1.27	–	1.50
		$F_{b,d,Rd-}$ [$\gamma_{M2} = 1.00, f_u = R_m$] / $F_{b,d,Rd-}$ [$\gamma_{M2} = 1.00, f_u = f_{uk}$]	0.98	1.19	1.27	–	1.50
12	Test vs design values with $f_u = f_{uk}$	$F_{b,exp+}$ / $F_{b,d,Rd+}$	1.37	1.26	1.43	1.26	1.86
		$F_{b,exp-}$ / $F_{b,d,Rd-}$	1.87	1.23	1.71	1.55	2.19
13	Test vs design values with $f_u = R_m$	$F_{b,exp+}$ / $F_{b,d,Rd+}$	1.40	1.06	1.13	–	1.24
		$F_{b,exp-}$ / $F_{b,d,Rd-}$	1.91	1.04	1.35	–	1.46
14	Test values: tensile vs compression bearing resistance	$F_{b,exp-}$ / $F_{b,exp+}$	1.42	1.01	1.24	1.23	1.24
		$F_{b,d,Rd-}$ / $F_{b,d,Rd+}$	1.04	1.03	1.04	1.00	1.05

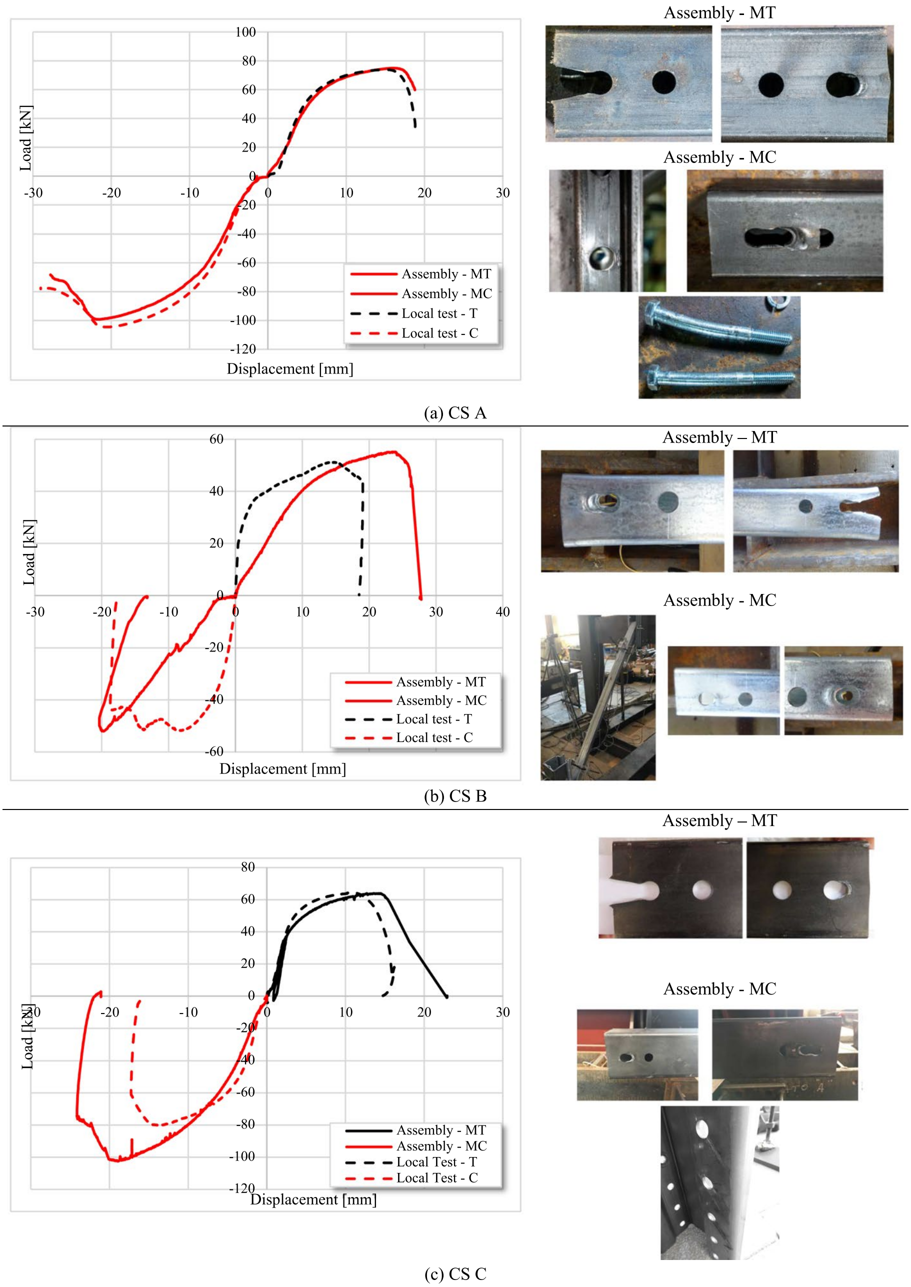

Fig. 16 *Assembly Tests* series—monotonic load: For the case studies A (**a**), B (**b**), C (**c**), D (**d**), E (**e**), force-displacement curves for monotonic tensile (MT) and compression (MC) loads and comparison with tensile (Local test—T) and compression (Local test—C) curves obtained from the local tests; failure modes for MT and MC tests

Journal : SmallCondensed 10518 | Article No : 1999 | Pages : 30 | MS Code : 1999 | Dispatch : 20-8-2024

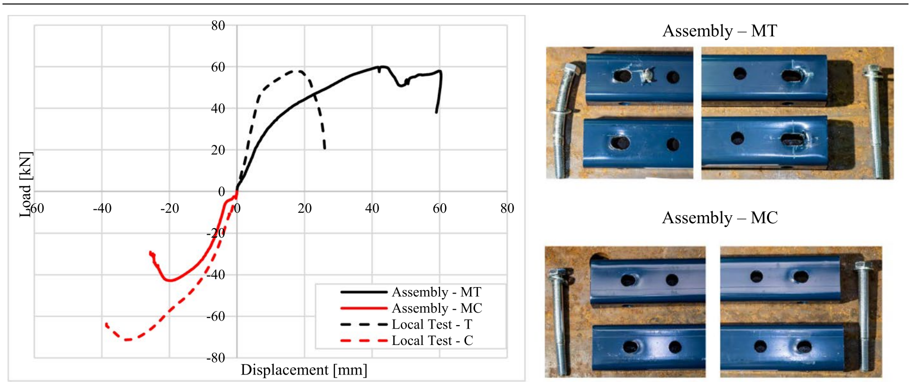

(d) CS D

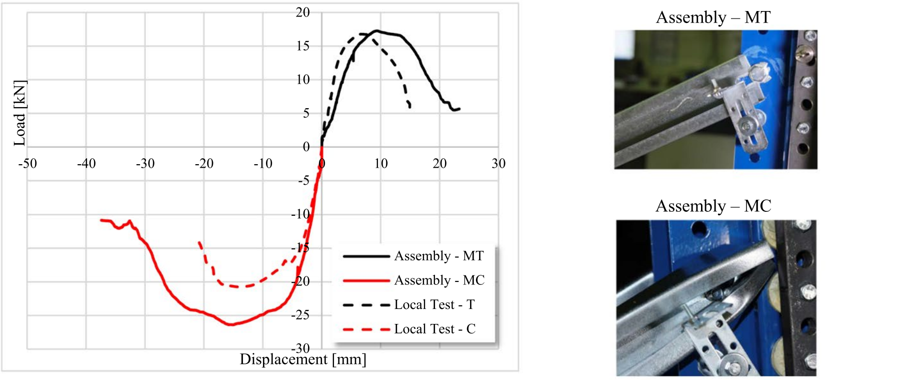

(e) CS E

Fig. 16 (continued)

In all cases, the final configuration of the diagonals is characterised by significant plastic ovalization in both the upper and the lower bolted connection. Web tearing in the diagonals is observed in some cases for tensile loading, while local buckling of the inner plate between the bolted and the empty hole in others for compression loading. Global buckling of the diagonal, when observed, occurs only after excessive damage in the connection (CS B, Fig. 16b).

In some cases, noteworthy differences can be observed between the Local and Assembly curves and thus need to be analysed from case to case due to the unique designer choices and peculiar geometrical characteristics of the selected components. Regarding the CS C (Fig. 16c), the assembly test demonstrates higher global resistance in compression. This can be attributed to the closure of the wings of the Ω upright section (see Table 1) during the application of the load and the consequent development of friction forces with the diagonal, as indicated by the scratches that were left from the contact of the diagonal with the upright. A similar over-resistance of the assembly compression curve can be noticed in CS E (Figs. 16e and 17). Looking at the global behaviour and the failure mode, this over-resistance is mainly due to the contact of the diagonal free end with the flanges of the upright (see Table 1).

Journal : SmallCondensed 10518	Article No : 1999	Pages : 30	MS Code : 1999	Dispatch : 20-8-2024

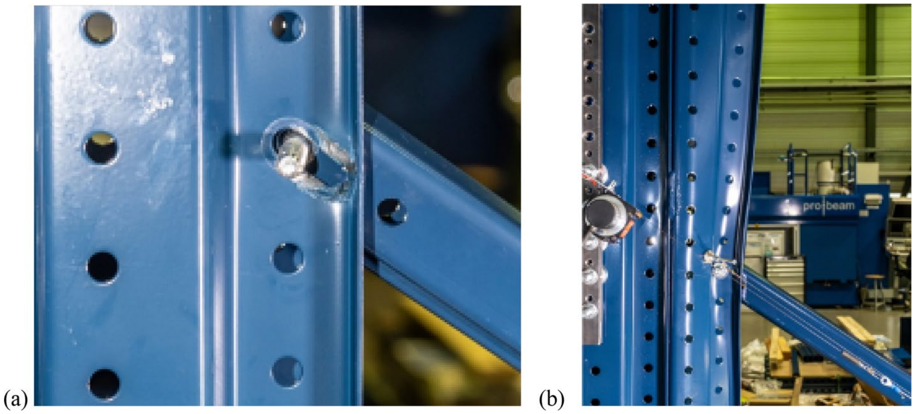

Fig. 17 *Assembly Tests* series—monotonic load, case study D. Focus on the deformation and damage of upright under (**a**) tension and (**b**) compression load

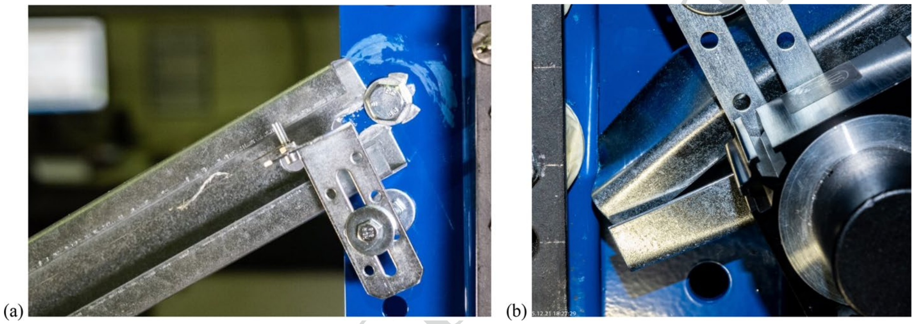

Fig. 18 *Assembly Tests* series—monotonic load, case study E: damage under tension load (**a**) and deformation of the diagonal and contact with the upright under compression load (**b**)

Finally, regarding the CS D (Fig. 16d and 18), the influence of the upright on the global behaviour of the assembly is clearly evident, both for tensile and compression load. In tension, bearing resistance is exceeded both in the diagonal and in the upright, (Fig. 18). In compression there is a clear distortion of the upright visible. Looking at the local and assembly force-deformation curves (Fig. 16d), while their resistances in tension are quite comparable, their stiffnesses are not: deformations are higher in the assembly test due to the ovalization of the upright's hole and the bolt bending. In compression, the assembly's resistance is lower than from the local test due to the strong local deformation of the upright profile.

5.2.2 Cyclic tests

The cyclic tests further confirm the behaviour observed in the monotonic tests, especially referring to the failure modes and to the localization of the damage. In case studies A, B, and C a very good correspondence among the backbones of the cyclic force-displacement curves and the monotonic ones can be noticed, with negligible loss of strength. For all case studies, pinching behaviour can be observed, due to the increasing looseness of the connection with the increase of plastic ovalization of the diagonal connection hole. In addition, for CS E a good correspondence between the monotonic and cyclic behaviour can still be observed, but with a higher variability of the cyclic response probably due to the high friction developed between the diagonal and the upright, testified by the lower pronounced pinching and the higher energy dissipated in each cycle (Fig. 19).

In the case of CS D, which was affected by a design mistake, strength degradation is quite relevant, and the developed failure mechanism involves not only the diagonal ends, but also (i) the upright hole, which experiences large plastic ovalization and (ii) the bolt, which is strongly bent. Bending of the bolt is amplified by the arrangement of the diagonals in this particular case study configuration: there are two C-section diagonal members in parallel, connected to the upright wings via a bolt that passes through the web plate of the profiles (Fig. 20a and Table 1). The initial looseness among the pieces and the progressive damage in both the diagonal and upright connections, caused the individual diagonal members to dislocate from their original position and move towards one another (Fig. 20b). Thus, the bolt started to be subjected to a bending moment, which resulted in a significantly poor behaviour that deviated from the intended design of the assembly (Fig. 20c). These effects were amplified by the limited transversal and torsional stiffness of the upright profile which led to very extensive distortion increasing 2nd order effects.

5.2.3 Considerations regarding the capacity design of the mechanisms

Considering the target capacity design associated with the POS strategy, it can be observed that all case study structures behaved as intended, with the only exception of CS D, which is in any case affected by a design mistake previously highlighted (red values in Table 2). Table 8 gathers the values of:

- The diagonal bearing resistances $F_{b,d,Rd}$ for tension and compression;
- The upright bearing resistance $F_{b,u,Rd}$ for tension and compression;
- The bolt shear resistance $F_{v,Rd}$;
- The diagonal net section resistance $F_{n,Rd}$;

Calculated according to prEN1993-1-3:2019, Table 10.5 (2019) by considering a safety factor equal to 1.0. Moreover, the table contains the maximum load values obtained by the local and assembly tests. Excluding CS D, one can again notice the generally good correspondence between the maximum forces obtained by the local and the assembly tests, highlighting that the governing failure mechanism is the plastic ovalization of the diagonal.

Despite the aforementioned considerations around the under-estimation of the bearing resistance of the diagonal calculated according to the prEN1993-1-3:2019 formulas (Table 7), especially in compression, it seems that the POS capacity design rules still manage to achieve the desired hierarchy among the possible mechanisms of the connection and of the diagonal element. The minor ovalization of the upright hole that was observed in some cases could suggest to moderately increase the over-strength coefficient for the bearing resistance of the upright with respect to the one of the diagonal, which is presently set at 1.20 per Eq. (2). Moreover, constraining internally the bolt (e.g., by- diminishing the unconstrained length of the bolt appearing in Fig. 21) results in a more compact behaviour of the connection, stabilising the shape of the connected open profiles (diagonal and upright) and allowing the bolt to mainly work in shear (CS B). In case of not having this

Journal : SmallCondensed 10518 | Article No : 1999 | Pages : 30 | MS Code : 1999 | Dispatch : 20-8-2024

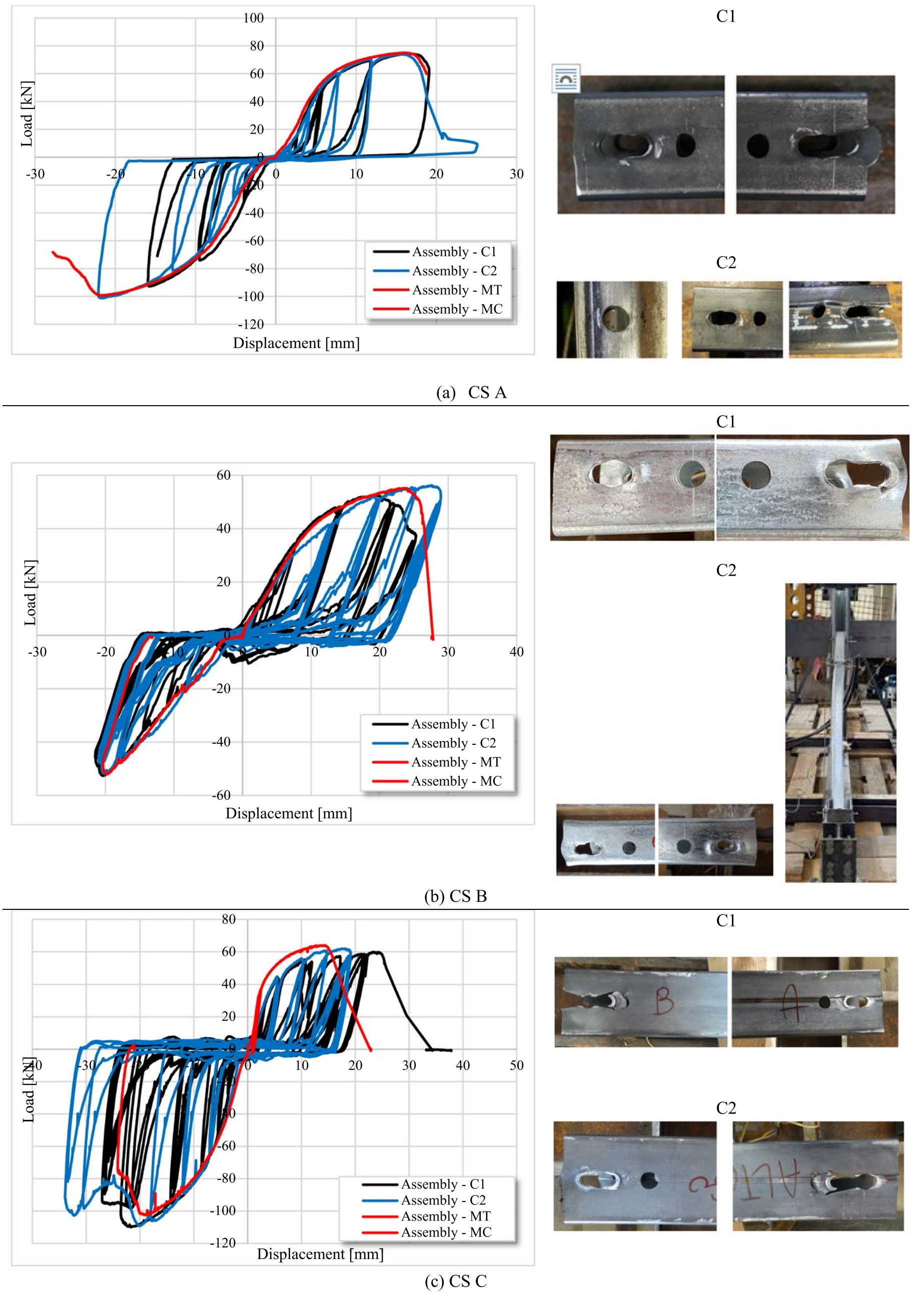

Fig. 19 *Assembly Tests* series – cyclic load: For the case studies A (**a**), B (**b**), C (**c**), D (**d**), E (**e**), force-displacement curves for cyclic test 1 (C1) and 2 (C2) loads and comparison with the monotonic load curves; failure modes for C1 and C2 tests

Journal : SmallCondensed 10518	Article No : 1999	Pages : 30	MS Code : 1999	Dispatch : 20-8-2024

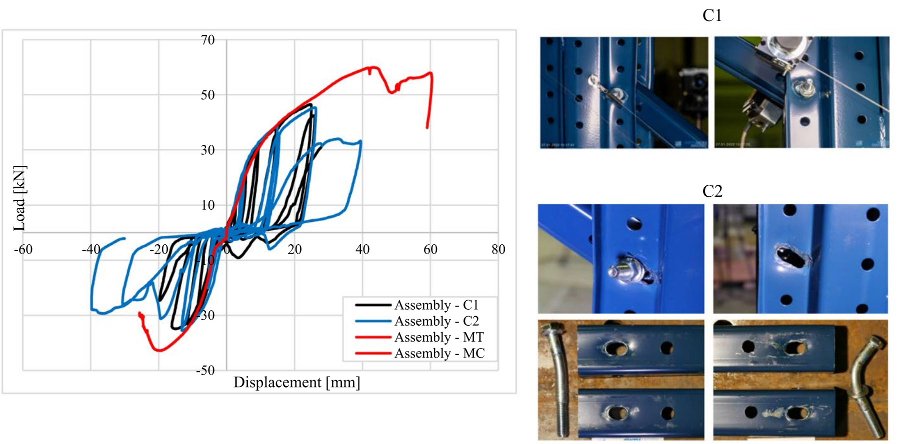

(d) CS D

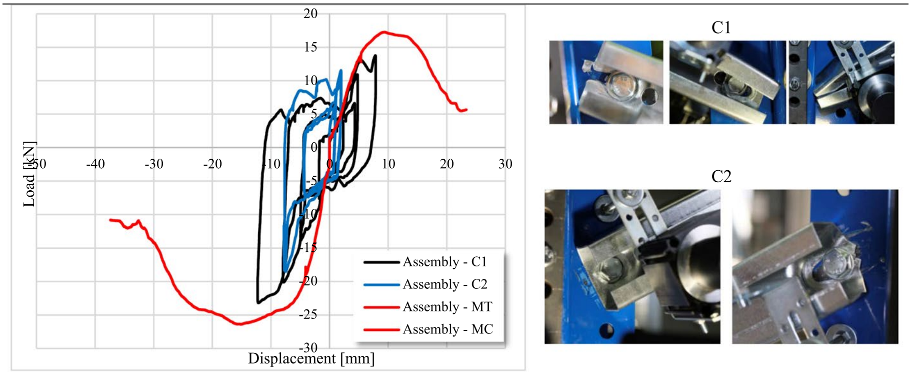

(e) CS E

Fig. 19 (continued)

internal constraint, diagonals working in parallel and connected through the web (CS D) should be avoided, as they can potentially lead to a poor, not symmetric, and unpredicted behaviour with increased damage accumulation.

6 Conclusions

This paper presents and discusses the experimental validation of the Plastic Ovalization Strategy (POS), a design strategy dedicated to the seismic design of racking structures, such as Rack Supported Warehouses (RSWs). This design approach is proposed for the one of the two main directions of the RSWs, which is made of consecutive adjacent trusses, each composed of two uprights connected by diagonals through bolts. The POS capacity design rules have been structured to concentrate damage and dissipation in the diagonal-to-upright connections through the plastic ovalization of the diagonal ends, while all the other failure mechanisms in the connection are prevented and all other elements remain in the elastic field. An additional bolt-less hole has been inserted in the inner-side of the diagonal, with the goal of controlling the bearing resistance in compression and make it comparable

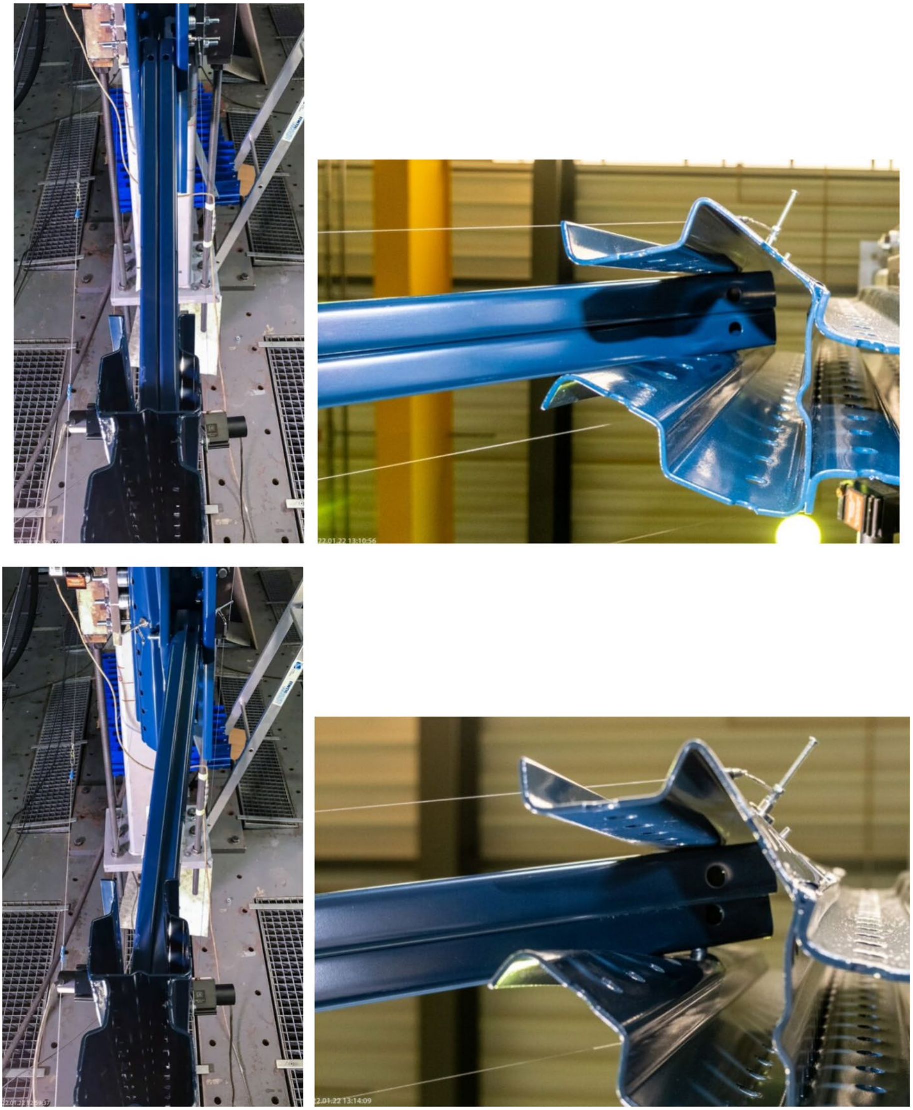

Fig. 20 Case Study D: progressive damage and movement of the diagonals during the test

to the one in tension. In this study, five sub-assemblies of diagonal-to-upright connections have been extracted from case study structures designed according to POS, to be tested according to two sets of tests: the *Local Tests*, to assess the actual bearing resistance of the diagonal connection with no other interferences; and the *Assembly Tests*, to evaluate the assembly behaviour and the over-resistance of the other mechanisms and elements.

In the Local Tests, both monotonic tensile and compressive loads are applied. In both cases, looking at the final configuration of the diagonals (Figs. 13b and 14b), it is clear that the connections fail in a ductile manner, exceeding the bearing resistance with relevant ovalization of the hole. By comparing the maximum force of the test with the

Journal : SmallCondensed 10518	Article No : 1999	Pages : 30	MS Code : 1999	Dispatch : 20-8-2024

Table 8 Main geometrical characteristics and resistance properties of the connections in the bottom part of the CS structures

Characteristics of the connection		CS A	CS B	CS C	CS D	CS E
Resistance values from Eurocode formula with $\gamma_{m2} = 1.00$	$F_{b,d,Rd+}$[kN]	53.75	40.60	45.00	45.90	9.00
	$F_{b,d,Rd-}$[kN]	55.90	42.00	46.80	45.90	9.45
	$F_{b,u,Rd+}$[kN]	165.00	100.80	100.80	41.25	43.20
	$F_{b,u,Rd-}$[kN]	165.00	100.80	100.80	41.25	43.20
	$F_{v,Rd}$[kN]	81.43	81.43	81.43	40.72	40.72
	$F_{n,Rd}$[kN]	207.05	103.49	166.31	144.06	55.49
Bearing resistance values from Local tests	$F_{b,d,LT+}$[kN]	73.85	51.31	64.37	57.99	16.77
	$F_{b,d,LT-}$[kN]	104.59	51.79	80.13	71.31	20.74
Maximum forces from Assembly tests monotonic load	F_{max,AT_M+}[kN]	74.96	55.15	63.88	59.90	17.27
	F_{max,AT_M-}[kN]	111.17	52.06	102.55	42.83	26.39
Maximum forces from Assembly tests monotonic load	F_{max,AT_C1+}[kN]	74.22	52.45	59.85	46.50	17.37
	F_{max,AT_C1-}[kN]	101.32	52.63	109.92	34.90	26.37
	F_{max,AT_C2+}[kN]	73.89	56.22	61.95	45.32	17.00
	F_{max,AT_C2-}[kN]	101.16	52.05	109.18	35.55	25.49

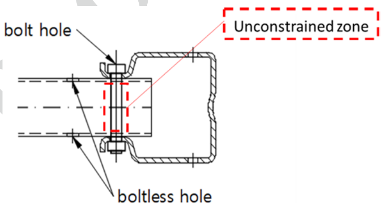

Fig. 21 Unconstrained zone of the bolt in the diagonal-to-upright connection

bearing resistance evaluated in the design according to prEN1993-1-3:2019 (Table 7), it seems that the Eurocode formula underestimates the value of the bearing resistance, this can be detrimental for the POS design where hierarchies among mechanisms must be respected to achieve the desired behaviour. Finally, the comparison between the bearing resistance in compression with the one in tension shows that although the addition of the boltless hole limits bearing resistance in compression and may help to control it, further investigations are needed for a more accurate evaluation of the actual bearing resistance in compression to be sure to respect the design requests and obtain the desired behaviour.

Regarding the Assembly tests, monotonic tensile and compression load, followed by with cyclic ones are applied. Excluding the one with an evident design mistake, the desired behaviour is generally observed, with the main damage localized in the diagonal-to-upright connection due to plastic ovalization of the diagonal, and little-to-no damage in the non-dissipative elements. Besides the generally observed behaviour, some case-to-case observations shall be done to limit the interference of the other components on the activation of the desired mechanism, as, for instance, constraining the internal zone of the connection to limit the out-of-plane deformation of the upright wings and avoiding the bolt bending, or avoiding unintended contact between elements that can increase the resistance in compression and lead to local damage.

The results of this experimental campaign highlight the capability of the POS capacity rules to guarantee the desired chain of failures in the diagonal-upright assembly, but also set the necessity for further investigations: (i) developing local structural models to better comprehend the local behaviour of the diagonal connection, and executing parametric analyses to appreciate how the geometrical parameters e_1, p_1 and the profile thickness affect the bearing resistance of the element and the observed damage; (ii) developing simplified models, starting from the local ones, to be inserted in the global case study structures models to check the global collapse mechanism for the final calibration of the POS design rules. In any case, the experimental campaign confirms the results numerically obtained within (Tsarpalis 2022), and together with the further investigations here listed highlights that POS can provide a new way of designing RSWs in seismic areas, founded on performance-based earthquake design, to be included in design codes as a fruitful easy-to-be-adopted alternative to design structurally safe RSWs, also under seismic action.

Author contributions Conceptualization: Dimitrios Vamvatsikos, Dimitrios Tsarpalis, Francesco Morelli, Agnese Natali; Methodology: Francesco Morelli, Agnese Natali, Dimitrios Vamvatsikos, Dimitrios Tsarpalis; Formal analysis and investigation: Francesco Morelli, Agnese Natali, Cristian Vulcu; Writing - original draft preparation: Agnese Natali; Writing - review and editing: Francesco Morelli, Cristian Vulcu, Dimitrios Tsarpalis, Dimitrios Vamvatsikos, Walter Salvatore, Benno Hoffmeister; Funding acquisition: Walter Salvatore, Ioannis Vayas; Supervision: Walter Salvatore, Dimitrios Vamvatsikos, Benno Hoffmeister, Ioannis Vayas.

Funding The authors are grateful for the funding provided by the EU Research Fund for Coal and Steel via the project "STEELWAR: Advanced structural solutions for automated STEELrack supported WAREhouses," Grant Agreement No. 754102.

Data availability The datasets generated during and/or analyzed during the current study are available from the corresponding author on reasonable request.

Declaration

Conflict of interests The authors have no relevant financial or non-financial interests to disclose.

References

BS EN 15512:2020 (2020a) Steel static storage systems. Adjustable pallet racking systems. Principles for structural design. In: https://www.en-standard.eu. https://www.en-standard.eu/bs-en-15512-2020-steel-static-storage-systems-adjustable-pallet-racking-systems-principles-for-structural-design/

Caprili S, Morelli F, Salvatore W, Natali A (2018) Design and analysis of automated rack supported warehouses. TOCIEJ 12:150–166. https://doi.org/10.2174/1874149501812010150

Cho Y, Teh LH, Ahmed A, Young B (2021) Material ductility and temperature effects on block shear capacity of bolted connections. J Constr Steel Res 177:106461. https://doi.org/10.1016/j.jcsr.2020.106461

Chung KF, Ip KH (2001) Finite element investigation on the structural behaviour of cold-formed steel bolted connections. Eng Struct 23:1115–1125. https://doi.org/10.1016/S0141-0296(01)00006-2

(1986) ECCS "Recommended testing procedure for assessing the behaviour of structural steel elements under cyclic loads"

(2020b) EN ISO 6892-1:2020—Metallic materials—Tensile testing. Part 1: Method of test at room temperature. https://store.uni.com/uni-en-iso-6892-1-2020. Accessed 21 Feb 2023

(2004) EN 1998-1:2004: Eurocode 8: Design of structures for earthquake resistance – Part 1: General rules, seismic actions and rules for buildings

(2016) BS EN 16681:2016 Steel static storage systems. Adjustable pallet racking systems. Principles for seismic design. In: https://www.en-standard.eu. https://www.en-standard.eu/bs-en-16681-2016-steel-static-storage-systems-adjustable-pallet-racking-systems-principles-for-seismic-design/

(2019) Eurocode 3—Design of steel structures—Part 1-3: General rules—Supplementary rules for cold-formed members and sheeting
(2021) Eurocode 3—Design of steel structures—Part 1-8: design of joints
Lyu Y-F, Wang Y-B, Li G-Q, Jiang J (2019) Numerical analysis on the ultimate bearing resistance of single-bolt connection with high strength steels. J Constr Steel Res 153:118–129. https://doi.org/10.1016/j.jcsr.2018.10.006
Natali A, Morelli F, Salvatore W (2022a) On the Seismic design and behavior of automated rack supported warehouse. Bull Earthq Eng 21(2):1081–1115
Natali A, Morelli F, Salvatore W, Tsarpalis D (2023c) Experimental validation of plastic ovalization strategy for seismic-resistant automated rack supported warehouses. Procedia Struct Integr 1(44):2326–2333
Natali A, Morelli F, Salvatore W (2022b) Seismic performance of currently designed automated rack supported warehouses. 7h world congress on civil, structural, and environmental engineering (CSEE'22)
Seleim S, LaBoube R (1996) Behavior of low ductility steels in cold-formed steel connections. Thin Walled Struct 25:135–151. https://doi.org/10.1016/0263-8231(95)00039-9
Suzuki Y, Lignos DG (2020) Development of collapse-consistent loading protocols for experimental testing of steel columns. Earthq Eng Struct Dyn 49(2):114–131
Tsarpalis P, Bakalis K, Thanopoulos P et al (2020) Pre-normative assessment of behaviour factor for lateral load resisting system FUSEIS pin-link. Bull Earthq Eng 18:2681–2698. https://doi.org/10.1007/s10518-020-00799-y
Tsarpalis D, Vamvatsikos D, Vayas I (2021) Seismic assessment approaches for mass-dominant sliding contents: the case of storage racks. Earthq Eng Struct Dyn n/a. https://doi.org/10.1002/eqe.3592
Tsarpalis D, Vamvatsikos D, Delladonna F et al (2022) Macro-characteristics and taxonomy of steel racking systems for seismic vulnerability assessment. Bull Earthq Eng. https://doi.org/10.1007/s10518-022-01326-x
Tsarpalis D (2022) "Ductile seismic design, performance assessment, and taxonomic characterization of steel racking systems", doctoral thesis, national technical university of athens, institute of steel structures
Vamvatsikos D, Bakalis K, Kohrangi M et al (2020) A risk-consistent approach to determine EN1998 behaviour factors for lateral load resisting systems. Soil Dyn Earthq Eng 131:106008. https://doi.org/10.1016/j.soildyn.2019.106008